Available online at www.sciencedirect.com

ScienceDirect

Procedia Structural Integrity 62 (2024) 1051–1060

Structural Integrity Procedia

www.elsevier.com/locate/procedia

II Fabre Conference – Existing bridges, viaducts and tunnels: research, innovation and applications (FABRE24)

Temperature effect on the modal frequencies of a steel railway bridge

Federico Ponsi[a], Ghita Eslami Varzaneh[b], Elisa Bassoli[b,*], Bruno Briseghella[b,c], Claudio Mazzotti[a], Loris Vincenzi[b]

[a]*Department of Civil, Chemical, Environmental, and Materials Engineering, University of Bologna, viale Risorgimento 2, Bologna, 40125, Italy*
[b]*Department of Engineering "Enzo Ferrari", University of Modena and Reggio Emilia, via Pietro Vivarelli 10, Modena, 41125, Italy*
[c]*College of Civil Engineering, Fuzhou University, Fuzhou, 350108, China*

Abstract

This paper presents the dynamic identification of the Ostiglia-Revere railway bridge, a steel truss girder bridge located in Northern Italy. The bridge is 6.6 m wide, about 940 m long and composed of 12 spans. The accelerations of a bridge span caused by both ambient excitation and train passages have been continuously measured from August to November. The monitoring system consists of 4 temperature sensors and 4 biaxial MEMS accelerometers, acquiring accelerations with a sampling frequency of 80 Hz. Modal properties are estimated adopting two different identification approaches, namely the Enhanced Frequency Domain Decomposition and the Stochastic Subspace Identification. Particular attention is paid to two crucial issues for vibration-based structural health monitoring: the recognition of the same structural mode from results identified during different time windows (i.e., mode clustering), and the temperature effect on estimated modal properties. As the latter is concerned, two regressive models, namely a linear regression model and an ARX model, are fitted to the frequency-temperature data, strongly reducing the eventuality of false vibration-based damage detections in the future.

Keywords: damage detection; temperature effects; vibration-based; structural health monitoring; railway bridge;

* Corresponding author. Tel.: +39 059 2056337; fax: +39 059 2056180.
E-mail address: elisa.bassoli@unimore.it

2452-3216
10.1016/j.prostr.2024.09.140

1. Introduction

Due to the vulnerability of built infrastructures, their functionality maintenance has recently become a priority concern in Italy and throughout Europe, as demonstrated by the Guidelines for the classification and management of risk, safety evaluation, and monitoring of existing bridges (MIMS, 2020) as well as by Eurocodes 1 and 3 of the European Committee for Standardization (EN 1991-2, 2003; EN 1993-1-9, 2005). Research in Structural Health Monitoring (SHM) and damage detection at the earliest possible stage is therefore rapidly expanding in the last few years, to prevent the huge economic losses caused by bridge regular service interruptions. In this context, vibration-based damage identification is attracting more and more attention and recognition (Avci et al., 2021). The basic idea behind this approach is that modal parameters (notably frequencies, mode shapes, and modal damping) are functions of the physical properties of the structure (mass, damping, and stiffness). Therefore, changes in the physical properties are expected to cause detectable variations in modal parameters, hence the importance of long-term monitoring systems.

However, in civil engineering structures and infrastructures, modal parameters are also influenced by ambient factors. Modal changes produced by environmental conditions, especially temperature variations, can be equivalent to or greater than the ones produced by damage. Therefore, it is necessary to distinguish between the variations in modal properties caused by structural damage from those simply due to environmental changes. The integration and interpretation of vibration and temperature data can be thus essential for the effectiveness of SHM in structural state assessment and damage detection. Otherwise, if the environment impact on the variation of dynamic parameters is not properly considered, vibration-based structural damage detection may produce false positive or negative damage alarms (Luo et al., 2022).

Although many experimental and theoretical studies have demonstrated the significance of temperature impact on structural vibration properties, it remains quite challenging to physically predict their dependence. It is widely recognized that a variation of the structure temperature leads to a modification of the material elastic modulus and thus to a change of the modal frequencies (Xia et al., 2012). However, temperature affects structures in a rather complicated manner. First, the thermal inertia might cause a temporal mismatch between cause and effect (Bassoli et al., 2017). Moreover, the non-uniform temperature distribution on large-scale structures produces non-homogeneous effects, other than the fact that solar irradiation is subject to fluctuations throughout the day and the seasons. Finally, temperature-induced changes in boundary conditions (e.g., support movements or variations in cable tension forces) are structurally dependent and extremely difficult to quantify (Alampalli, 1998). Therefore, it is quite evident that the task of finding a physical quantitative description of all the involved phenomena is far too complicated.

In light of this, ‘black box’ models are generally adopted (Peeters et al., 2001), where the term ‘black box’ means that no physical modeling is involved. The parameters of the ‘black box’ model are determined by fitting its results to the data, namely time series of measured temperatures and structural modal parameters, identified from recorded accelerations. The most simple approach to establish a model is by linear regression analysis, i.e., assessing a linear relation between temperature and modal frequency (evaluated at the same time instant) by least squares. More refined models do not simply correlate ‘static’ measures (i.e., simultaneous data taken off out of their background context) but are trained based on the thermal dynamics of the bridge, which is rather essential in case of cause-to-effect time shifts. The AutoRegressive model with eXogenous inputs (ARX) is possibly the most basic ‘dynamic’ model among those available in the literature (see, for instance, Wang et al., 2020). Preliminary results presented in this paper are based on linear regression and ARX ‘black box’ models, toward the definition of the temperature seasonal variation effects on the modal frequencies of a real-scale steel-concrete railway bridge. The aim is that, once the model is numerically calibrated on data collected during the long-term monitoring reference period, any change in modal parameters detected in future experimental acquisitions could be correctly attributed to temperature variations or actual damage occurrence.

In the following, the case study of the Ostiglia-Revere railway viaduct is presented and discussed. The bridge is 6.6 m wide and about 940 m long, subdivided into 12 spans composed of independent pairs of single span truss girders (one for each train lane), holding a concrete deck with lateral barriers for railway ballast containment. Results of the long-term monitoring system installed on an inner span are here reported, and particular attention is paid to the temperature effect on the estimated modal properties. Specifically, the paper is organized as follows. Section 2 briefly introduces the examined structure and illustrates the long-term dynamic monitoring conducted from August to

November through a network of wired-accelerometers and temperature sensors. Section 3 deals with the Operation Modal Analysis (OMA) techniques used for the vibration-based identification of the structure modal properties, on the basis of the recorded accelerations. In particular, the Stochastic Subspace Identification (SSI – Peeters and De Roeck, 1999) and the Enhanced Frequency Domain Decomposition (EFDD – Brincker et al., 2001) methods are adopted, and a clustering procedure is specifically designed to correctly organize derived modal parameters excluding outliers. Then, a linear regression and an ARX model are used in Section 4 to capture the relationship between modal parameters and environmental temperature. Finally, conclusions are drawn in Section 5.

2. Long-term dynamic monitoring of the Ostiglia-Revere viaduct

The Ostiglia-Revere viaduct is a steel-concrete viaduct located close to Mantova (Italy), crossing the Po River on the Bologna–Verona railway line (see Fig. 1). The structure is managed by the Italian Railway Network (RFI) and holds the record for being the longest steel railway bridge in Italy, with a total length of about 940 m. The river crossing takes place through two parallel railway viaducts (accommodating the two opposite train tracks), each composed of twelve spans: eight being 73.6 m long and four 64.4 m long. Each span is composed of two parallel steel trusses, completed by a concrete deck. Trusses are identical and completely independent from each other; they are composed of π-shaped upper and lower chords and H-shaped diagonals and girders, bolted together at the joints. Systems of upper and lower horizontal braces are also provided. Steel elements are different from each other and specifically designed according to the geometry of the respective span. Longitudinal girders are meant to carry cross girders in support of the train tracks, as well as a concrete deck provided with lateral barriers to contain the ballast.

The long-term dynamic monitoring covers the period between August and November, during which data is acquired in a continuous manner, including environmental condition and train passages. To present preliminary results, only the monitoring of a single viaduct span is considered. In particular, an inner span of 73.6 m is selected for logistic reasons, including the simple access to electricity. Moreover, given their identical nature, only one of the two parallel trusses of the span is dealt with. Three key span sections are instrumented to be monitored, namely one-quarter, mid-span, and three-quarters. Each section is provided with a temperature sensor and a biaxial MEMS accelerometer (Guidorzi et al., 2010; Bassoli et al., 2015) recording accelerations in the vertical and (transverse) horizontal directions, to identify both vertical and lateral bending modes. In addition, at the mid-span section, a temperature sensor and a

(*a*) (*b*)

Fig. 1. Ostiglia-Revere viaduct: (a) top view and (b) example span street view from Google Earth.

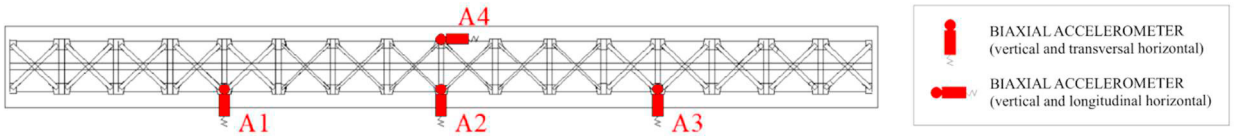

Fig. 2. Accelerometer network set-up on the examined span (view from lower braces).

biaxial MEMS accelerometer are also placed in the parallel truss, recording along vertical and (longitudinal) horizontal directions, to also detect longitudinal and torsional deformations. Fig. 2 shows the set-up of the four accelerometers, all applied by magnets at the joints between diagonals and lower chord. In this regard, it is recalled that the location of temperature sensors matches that of accelerometers.

3. Operational modal analysis

To analyze free vibrations with a high signal-to-noise ratio, time windows right after train passage are selected. Particular attention is paid to the windows selection, since the mass of the train would have a non-negligible impact on the system modal mass. Accordingly, examined time per month narrows from 43200 or 44640 minutes (in case of months with 30 or 31 days, respectively) to approximatively 1500-1700 minutes depending on the considered month. Starting with acceleration recordings following the train span leave, two OMA algorithms are implemented for modal properties identification, namely the SSI (Peeters and De Roeck, 1999) and the EFDD (Brincker et al., 2001) methods. Once all selected time windows are examined and modes are extracted by either the SSI or the EFDD methods, a clustering procedure is then used for their grouping as well as for outlier discarding. In this, each month is treated separately, distinguishing between SSI and EFDD outcomes. For each identified mode, a vector (9 components) containing the modal frequency and the corresponding one-normalized mode shape (8 components, being four the biaxial accelerometers) is arranged. The MATLAB algorithm Density-Based Spatial Clustering of Applications with Noise (DBSCAN) of Ester et al. (1996) is used, which identifies clusters (referred to as core points) and outliers (noise points) based on two input parameters: neighborhood search radius around the nine-dimensional point and minimum number of neighbors required for assessing a cluster. Afterwards, clusters that fail to maintain stability for all months are rejected.

Six clusters and hence modes are established by the DBSCAN of both EFDD and SSI outcomes. In the following, only modes identified from the clustering of EFDD results are presented and discussed, as modes derived from the SSI lead to very similar conclusions. In August, for instance, 4900 modes are identified from the EFDD modal analysis (considering all time windows right after the train crossing), of which only 3532 are clustered by the DBSCAN

Table 1. EFDD mode clusters: median natural frequency f_{med} (Hz), mean MAC between mode shapes and their median (-), population Pop. (-).

Mode Nr.	August			September			October			November			Overall period		
	f_{med}	MAC	Pop.	f_{med}	MAC	Pop.	f_{med}	MAC	Pop.	f_{med}	MAC	Pop.	f_{med}	MAC	Pop.
1	1.67	0.96	1044	1.68	0.99	694	1.69	0.99	939	1.70	0.99	787	1.69	0.98	3464
2	2.99	0.95	1062	2.99	0.99	590	3.00	0.99	659	3.00	0.99	572	2.99	0.97	2883
3	3.45	0.96	885	3.46	0.99	530	3.47	0.99	682	3.48	0.99	655	3.47	0.98	2752
4	4.51	0.92	266	4.54	0.98	157	4.56	0.98	128	4.59	1.00	162	4.55	0.94	713
5	6.17	0.93	118	6.20	0.98	26	6.19	0.97	43	6.25	0.98	45	6.19	0.85	232
6	8.74	0.92	157	8.77	0.98	94	8.79	0.98	97	8.82	0.98	98	8.78	0.95	446

Table 2. Range of estimated natural frequencies (EFDD clustering): minimum and maximum values (in Hz) over months and overall period.

Mode Nr.	August		September		October		November		Overall period	
	f_{min}	f_{max}	f_{min}	f_{max}	f_{min}	f_{max}	f_{min}	f_{max}	f_{min}	f_{max}
1	1.65	1.70	1.67	1.70	1.67	1.71	1.68	1.72	1.65	1.72
2	2.94	3.01	2.96	3.01	2.96	3.02	2.97	3.02	2.94	3.02
3	3.41	3.50	3.45	3.48	3.45	3.50	3.46	3.49	3.41	3.50
4	4.46	4.58	4.50	4.58	4.52	4.60	4.55	4.63	4.46	4.63
5	6.11	6.25	6.15	6.23	6.15	6.26	6.19	6.29	6.11	6.29
6	8.66	8.81	8.73	8.84	8.73	8.85	8.79	8.85	8.66	8.85

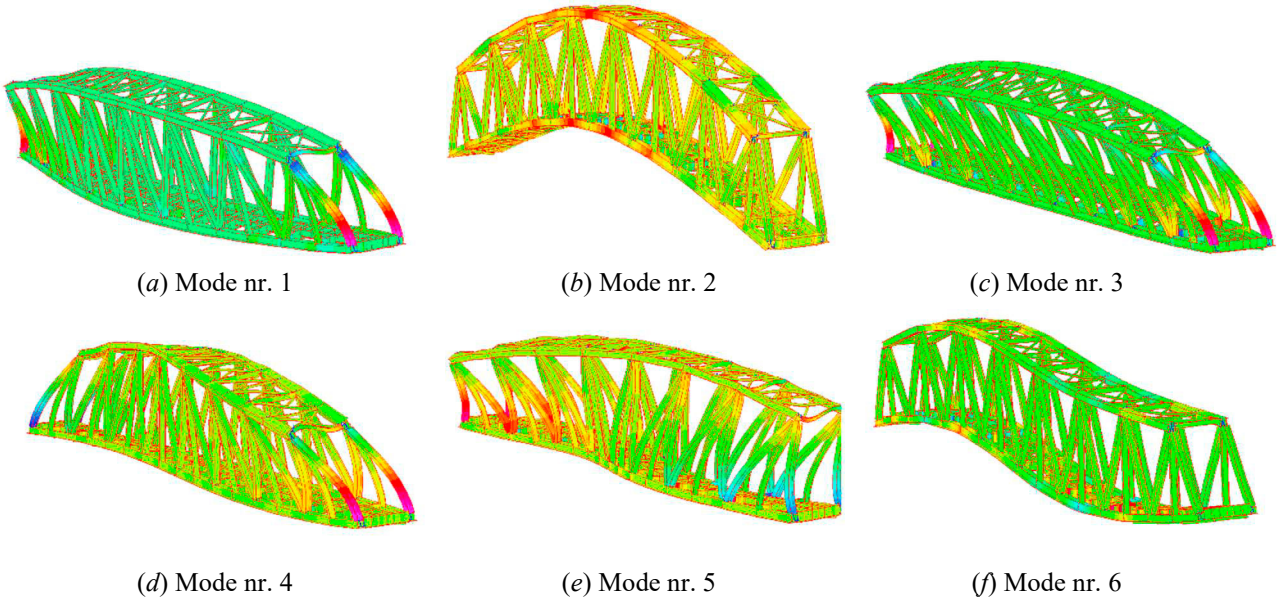

(*a*) Mode nr. 1 (*b*) Mode nr. 2 (*c*) Mode nr. 3

(*d*) Mode nr. 4 (*e*) Mode nr. 5 (*f*) Mode nr. 6

Fig. 3. Mode shapes resulting from the developed Finite Element Model (FEM) and coupled to the 6 identified experimental modes shapes.

within the six modes, leading to a total discard percentage of outlier of about 27.9 %. Similar considerations also apply to September, October and November.

Then, the centroid of mode clusters is evaluated as the data median along all the nine dimensions (one natural frequency and eight mode shape components). Modal clusters established both monthly and globally by the DBSCAN of EFDD modes are presented in Table 1, containing the number of EFDD mode vectors grouped together within each cluster, median natural frequency (f_{med}), and average Modal Assurance Criterion (MAC) calculated among all mode shapes and their median. Moreover, Table 2 lists the range (i.e., minimum and maximum values) of natural frequencies clustered within the same mode. Actually, some modal clusters with natural frequency between 6.3 and 8.5 Hz are also identified by the DBSCAN, but ultimately discarded due to their lack of stability over months. To provide an immediate graphic representation of identified mode shapes, a Finite Element Model (FEM) developed in Straus7 is exploited, resulting in Fig. 3.

To comment briefly on the mode shapes, it should be specified that the Ostiglia-Revere viaduct was specifically designed to mainly support vertical loads. Due to the presence of the vertical truss girders, the bridge has a high stiffness in the vertical plane, but it is more deformable in the transverse direction. Moreover, the non-structural concrete deck might further stiffen vertical deflections. Therefore, the first mode shows a symmetric horizontal transversal deformation of the bridge. The second mode is a bending mode with symmetric deflection along the vertical axis. The third mode features a horizontal (transversal) torsional deformation. The fourth and the fifth are both transverse horizontal with anti-symmetric deformation and significant cross-section distortion. Lastly, the sixth mode develops along the vertical direction, being an anti-symmetric bending mode.

4. Effect of the temperature on the modal properties

In this section, the obtained frequencies are examined *vs* temperature values, to analyze the impact of environmental effects on the viaduct modal properties. Each time window subject to OMA is coupled with the ambient temperature recorded, calculated as the average among those provided by the four sensors. Therefore, each mode identified by the EFDD method and clustered by the DBSCAN is linked to its own outside temperature value. Monthly mean, minimum, and maximum temperature values are listed in Table 3, together with the same quantities related to the overall monitoring period.

Table 3. Recorded temperatures: mean, minimum, and maximum values (in °C) over months and overall period.

August			September			October			November			Overall period		
T_{mean}	T_{min}	T_{max}	T_{mean}	T_{min}	T_{max}	T_{mean}	T_{min}	T_{max}	T_{mean}	T_{min}	T_{max}	T_{mean}	T_{min}	T_{max}
31.8	21.5	40.8	23.8	17.3	33.0	20.7	14.0	27.5	14.1	7.0	21.5	23.6	7.0	40.8

First, monthly analyses for each mode are conducted to observe daily fluctuations. For instance, the case of the third mode in August and October is here reported as an example, as illustrated in Fig. 4: the first row shows the EFDD frequency data clustered by the DBSCAN within the third mode, each corresponding to its respective acceleration recording time, whereas the second row illustrates the time-series of the temperature (average between the four sensors). Such a comparison reveals a general anti-phase between estimated modal frequency and outside temperature: an increase in temperature returns an almost immediate decrease in modal frequency, implying no temporal mismatch between cause and effect. This is perfectly in line with expectations, since steel structures typically do not suffer from thermal inertia. The same considerations also apply to the other five modes, as well as in case SSI rather than EFDD outcomes are considered.

Then, the entire monitoring period is considered. Fig. 5 shows the EFDD natural frequencies clustered within four selected modes *vs* temperature (black dots). Specifically, the first two horizontal modes (nr. 1 and 3) and the first two bending modes (nr. 2 and 6) are reported. The remaining two modes (nr. 4 and 5) are not showed but they follow

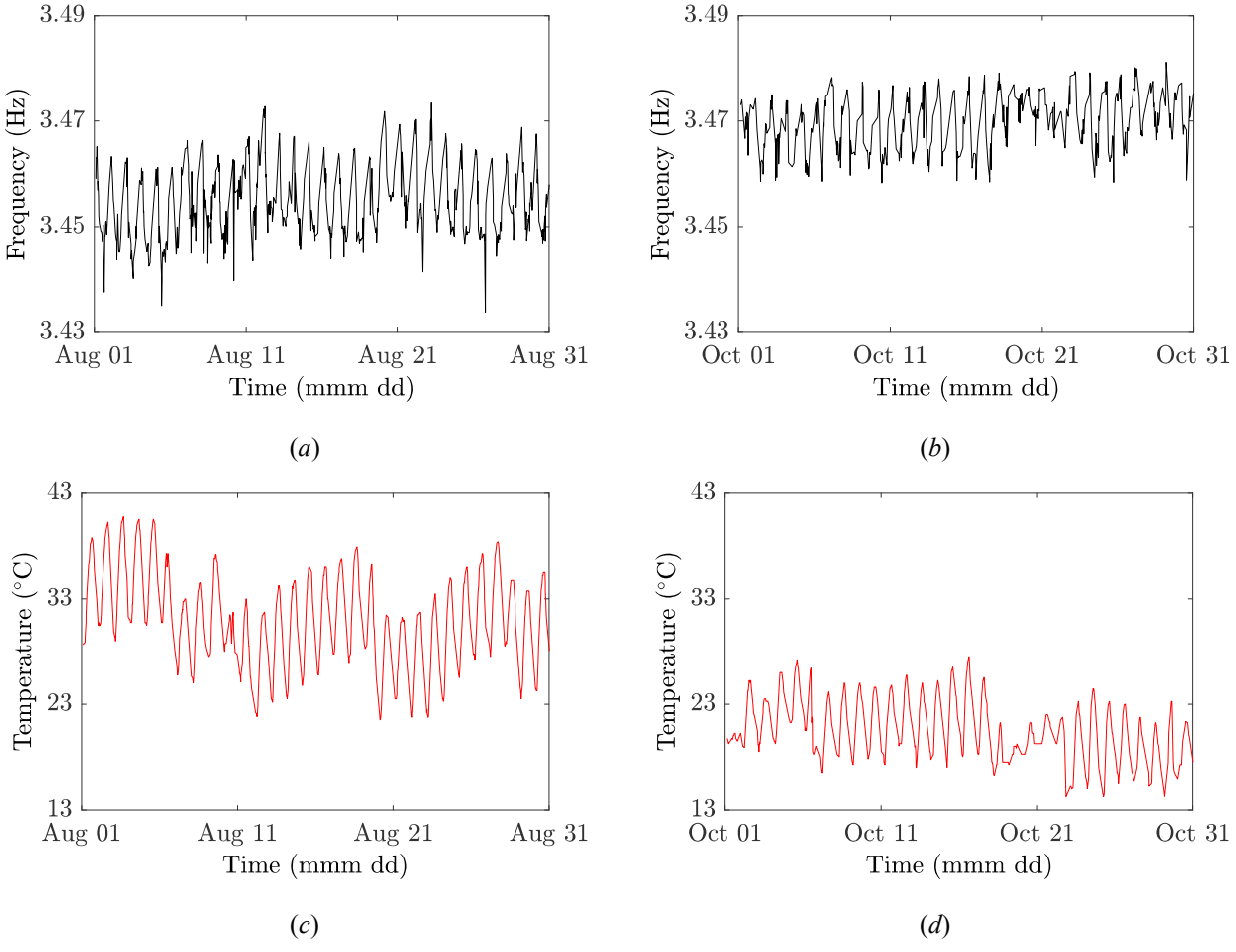

Fig. 4. Third mode clustered by the DBSCAN: natural frequencies identified by the EFDD method from recorded accelerations (first row) and relative temperatures (second row) versus time, during the reference months of August (first column) and October (second column).

similar trend. The analysis shows that modes are differently affected by temperature, especially as regards the second mode which appears to be slightly dependent of it. Anyway, the natural frequency f (Hz) of all mode follows a (more or less marked but) quite linear temperature-dependent trend, clearly evident even in case of sparsely populated modes (e.g., the sixth mode). This suggests the effectiveness of a linear regression analysis for all the identified modes.

For each mode, a linear fitting based on least squares is therefore conducted, reading:

$$f(T) = m\left(T - T_{ref}\right) + c, \tag{1}$$

where T_{ref} = 20 °C is the reference temperature, m is the slope (Hz/°C), and c is the frequency when the temperature is T_{ref}. For the four modes considered, regressions provide the red lines of Fig. 5. Calibrated m and c parameters are listed in Table 4 for all the six modes, together with the standard error in frequency estimation σ_f (Hz). The unevenness of the modal slopes m further demonstrates conclusions qualitatively drawn above, namely the non-homogeneous temperature effect on modes in the specific case of application. This is especially valid for the second mode, whose calibrated slope is of an order of magnitude lower than those of the other modes (see Table 4).

Based on the standard error σ_f (Hz) of Table 4, the 95% prediction interval of natural frequencies can be assessed as the $f(T)$ estimate of Eq (1) plus or minus $2\,\sigma_f$, leading to the gray dashed lines of Fig. 5. In this way,

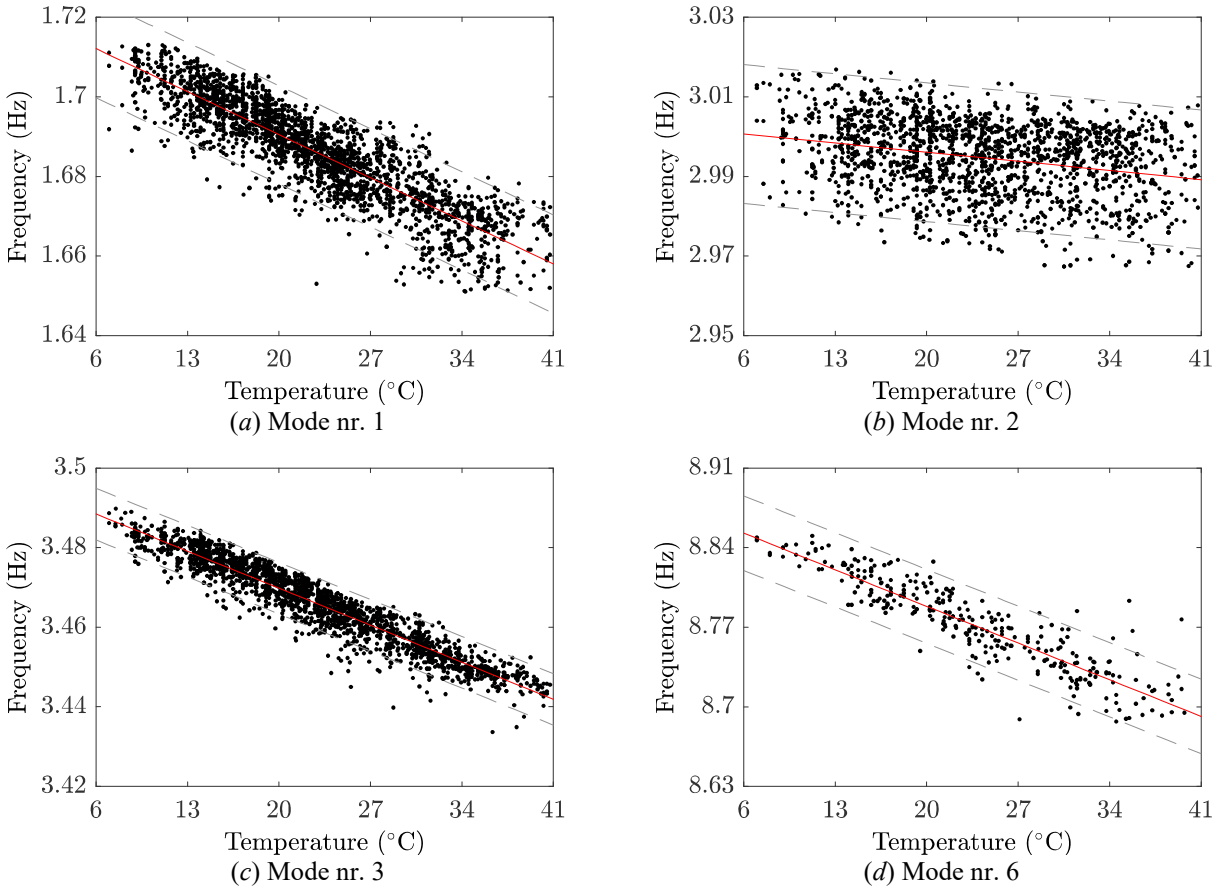

Fig. 5. Four example modes clustered by the DBSCAN: natural frequencies identified by the EFDD method from recorded accelerations versus corresponding outside temperature (black dots), overlaid with calibrated linear regressions (red lines), and 95% prediction intervals (grey dashed lines).

Table 4. Linear regression analysis: calibrated parameters and standard error.

	Mode nr. 1	Mode nr. 2	Mode nr. 3	Mode nr. 4	Mode nr. 5	Mode nr. 6
$m \cdot 10^3$ (Hz/°C)	-1.55	-0.33	-1.33	-3.99	-4.57	-4.60
c (Hz)	1.69	3.00	3.47	4.56	6.22	8.79
σ_f (Hz)	0.0062	0.0087	0.0032	0.0104	0.0190	0.0162

future evaluations can be potentially assessed as conditions that require attention by accounting for the statistical properties of the linear model prediction. This is meant to avoid false detection, i.e., to easily understand whether or not natural frequency deviations to median values established during the long-term monitoring period (see Table 2) are simply due to temperature.

To assess the appropriateness of the linear regressive (LR) model, a more sophisticated method coming from the system identification literature (Guidorzi, 2003) is also implemented. In particular, the ARX model is adopted, consisting in the combination of an auto-regressive output (AR) and an exogeneous input (X) part:

$$f_k + a_1 f_{k-1} + \cdots + a_{n_a} f_{k-n_a} = b_1 T_{k-n_k} + b_2 T_{k-n_k-1} + \cdots + b_{n_b} T_{k-n_k-n_b+1} + e_k, \quad (2)$$

where f_k is the output (in this case a natural frequency) at time instant k, T_k is the input (in this case a temperature), and e_k is the error term modelling the white-noise disturbances that act on the input–output process. Parameters n_a and n_b are the orders of the ARX model, while n_k is the pure time delay between input and output, here set at zero as no thermal inertia is observed in the case of study (see Fig. 4). For each mode, the ARX model is established by a MATLAB routine with $[n_a, n_b, n_k] = [4, 2, 0]$, trained with temperatures (inputs) and natural frequencies (outputs) acquired during the whole monitoring period.

The predictions of LR and ARX models are illustrated in Fig. 6, showing the case of the third mode in the months of August and October. As demonstrated in Table 5, the ARX model provides standard error values 50% smaller than those provided by the LR approach. However, standard errors of the LR model are deemed to be satisfactory, especially considering the extreme simplicity of the method. Moreover, the linear regression applicability to future data is more immediate, as the temperature-to-eigenfrequency relation correlates simultaneously measured data, without the need to know the history behind those measurements.

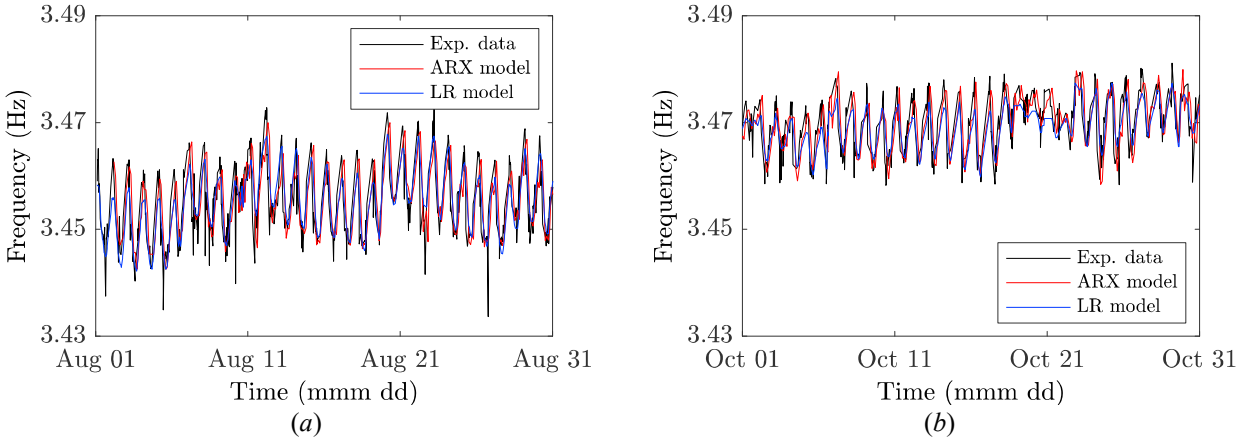

Fig. 6. Comparison between experimental data (in black), LR (in red) and ARX (in blue) model predictions: example case of the third natural frequency during the months of August (a) and October (b).

Table 5. Comparison of standard error (Hz) between ARX and LR models.

	Mode nr. 1	Mode nr. 2	Mode nr. 3	Mode nr. 4	Mode nr. 5	Mode nr. 6
LR model	0.0062	0.0087	0.0032	0.0104	0.0190	0.0162
ARX model	0.0039	0.0063	0.0022	0.0051	0.0038	0.0108

5. Conclusions

In this paper, a real case application of vibration-based monitoring is presented and discussed. The examined structure consists in the Ostiglia-Revere viaduct built close to Mantova (Italy), a steel-concrete structure allowing the Bologna-Verona railway line to cross the Po River. A four-month long-term monitoring was conducted on a reference single span, based on a wired-accelerometer network paired with temperature sensors. The accelerations of the span caused by both ambient excitation and train crossing were continuously measured from August to November, but only data following the train transit on the railway are selected, to concentrate the analysis on the free vibrations of the bridge with high signal-to-noise ratio.

Two OMA techniques are used to extract structural modal properties from acquired accelerations, one in frequency (EFDD) and one in time (SSI) domains. Results are organized in clusters thanks to the DBSCAN, which helps finding similar modes and outliers. In the specific case, the same weight on frequency and mode shape components is foreseen. Then, only clusters that recur in every month of monitoring are selected. Six modes are thus experimentally determined, whose modal parameters are evaluated as the median of modes grouped together within the cluster.

Finally, the trend of modes is analyzed versus temperature. Herein, presented results are limited to modes coming from the clustering of EFDD outcomes, but SSI clusters lead to very similar conclusions. By considering two months as a reference, daily fluctuations of modal frequencies (due to the excursion temperature between day and night) result quite evident. An increase of the ambient temperature generates a reduction of modal frequencies, as typical for steel structures. Moreover, no misalignment between the variations of temperature and modal frequencies occurs, implying that no thermal inertia affects the structure.

The entire monitoring period is then investigated, to catch the seasonal effect of temperatures on modes. Modal frequencies follow an almost linear pattern with temperature; hence, a ‘black box’ linear regression is used to analytically describe the temperature-dependence of modes. Modes turn out to be differently affected by the ambient temperature. Specifically, the most temperature-dependent mode is the sixth, and the second mode is the least affected by temperature variations. Anyway, once the linear regression model is calibrated for each mode separately, based on data acquired during the monitoring period, future recordings can be cleared of temperature effects, to avoid false vibration-based damage detections. The linear regression method is compared to the ARX model, a more refined data-driven system identification approach, calibrated based on recorded temperatures and natural frequencies. As expected, the ARX model, which includes the thermal dynamics of the bridge, provides more accurate predictions than the ‘static’ regression model. However, despite being simpler by nature, the linear regression also returns satisfactory results in predicting natural frequencies based on temperature.

Acknowledgements

This study was carried out within the RETURN Extended Partnership and received funding from the European Union Next-GenerationEU (National Recovery and Resilience Plan – NRRP, Mission 4, Component 2, Investment 1.3 – D.D. 1243 2/8/2022, PE0000005).

References

Alampalli, S., 1998. Influence of in-service environment on modal parameters. In Proceedings of the 16th International Modal Analysis Conference. Santa Barbara, California, Vol. 1: pp. 111–116.

Avci, O., Abdeljaber, O., Kiranyaz, S., Hussein, M., Gabbouj, M., Inman, D. J., 2021. A review of vibration-based damage detection in civil structures: From traditional methods to Machine Learning and Deep Learning applications. Mechanical Systems and Signal Processing, 147, 107077.

Bassoli, E., Vincenzi, L., Bovo, M., Mazzotti, C., 2015. Dynamic identification of an ancient masonry bell tower using a MEMS-based acquisition system. 2015 IEEE Workshop on Environmental, Energy, and Structural Monitoring Systems, EESMS 2015, pp. 226–231.

Bassoli, E., Forghieri, M., Bovo, M., Mazzotti, C., Vincenzi, L., 2017. The role of environmental effects in the structural health monitoring: the case study of the Ficarolo Tower in Rovigo. In Proceedings of XVII ANIDIS Conference. Pistoia, Italy, pp. 154–162.

Brincker, R., Ventura, C. E., Andersen, P., 2001. Damping estimation by frequency domain decomposition. In Proceedings of IMAC 19: A Conference on Structural Dynamics. Kissimmee, Florida, pp. 698–703.

EN 1991-2, 2003. Eurocode 1: Actions on structures – Part 2: Traffic loads on bridges. European Committee for Standardization.

EN 1993-1-9, 2005. Eurocode 3: Design of steel structures – Part 1-9: Fatigue. European Committee for Standardization.

Ester, M., H.-P. Kriegel, J. Sander, X. Xiaowei, 1996. A density-based algorithm for discovering clusters in large spatial databases with noise. In Proceedings of the Second International Conference on Knowledge Discovery in Databases and Data Mining. Portland, Oregon, pp. 154–162.

Guidorzi, R., 2003. Multivariable System Identification, Bonomia University Press, Bologna.

Guidorzi, R., Diversi, R., Vincenzi, L., Simioli, V., 2010. MEMS-based sensing for health monitoring of buildings. Fifth European Workshop on Structural Health Monitoring, pp. 901-906.

Luo, J., Huang, M., Lei, Y., 2022. Temperature Effect on Vibration Properties and Vibration-Based Damage Identification of Bridge Structures: A Literature Review. Buildings 12(8), 1209.

Italian Ministry for Sustainable Infrastructure and Mobility (MIMS), 2022. Guidelines for the classification and management of risk, safety evaluation, and monitoring of existing bridges (in Italian). n. 54/2022 C.S.LL.PP., Rome, Italy.

Peeters, B., De Roeck, G., 1999. Reference-based stochastic subspace identification for output-only modal analysis. Mechanical Systems and Signal Processing 13(6), 855–878.

Peeters, B., Maeck, J., De Roeck, G., 2001. Vibration-based damage detection in civil engineering: excitation sources and temperature effects. Smart Materials and Structures 10(3), 518.

Wang, Z., Huang, M., Gu, J., 2020. Temperature effects on vibration-based damage detection of a reinforced concrete slab. Applied Sciences 10(8), 2869.

Xia, Y., Chen, B., Weng, S., Ni, Y. Q., Xu, Y. L., 2012. Temperature effect on vibration properties of civil structures: a literature review and case studies. Journal of Civil Structural Health Monitoring 2, 29-46.